Published in final edited form as:
J Card Fail. 2011 March ; 17(3): 253–263. doi:10.1016/j.cardfail.2010.10.008.

Left Ventricular Dysfunction in Murine Models of Heart Failure and in Failing Human Heart is Associated With a Selective Decrease in the Expression of Caveolin-3

Ellina Cheskis Feiner, MD[1], **Paul Chung, MD**[1], **Jean Francois Jasmin, PhD**[2], **Jin Zhang, PhD**[1], **Diana Whitaker-Menezes, MS**[2], **Valerie Myers, BS**[1], **Jianliang Song, MD, PhD**[1], **Elizabeth W. Feldman**[1], **Hajime Funakoshi, MD, PhD**[1], **Brent R. DeGeorge Jr., PhD**[1], **Rao V. Yelamarty, PhD**[3], **Walter J. Koch, PhD**[1], **Michael P. Lisanti, MD, PhD**[2], **Charles F. McTiernan, PhD.**[4], **Joseph Y. Cheung, MD, PhD**[1], **Michael R. Bristow, M.D., Ph.D**[5], **Tung O. Chan, PhD**[1], and **Arthur M. Feldman, MD, PhD**[1]

[1] Department of Medicine, Center for Translational Medicine, Thomas Jefferson University, Philadelphia, PA

[2] Department of Cancer Biology, Thomas Jefferson University, Philadelphia, PA

[3] LASERVY Corporation

[4] University of Pittsburgh School of Medicine, Pittsburgh, PA

[5] University of Colorado Health Sciences Center, Denver, CO

Abstract

Caveolin are scaffolding proteins that are integral components of caveolae, flask shaped invaginations in the membranes of all mammalian cells. Caveolins-1 and −3 are expressed ubiquitously whereas caveolin-3 is found only in muscle. The role of caveolin-3 in heart muscle disease is controversial. The present study was undertaken to assess the effects of left ventricular dysfunction on the expression of caveolin proteins using two well-characterized models of murine heart failure and failing human heart. Mice with constitutive overexpression of A_1-adenosine receptor (A_1-TG) demonstrate cardiac dilatation and decreased left ventricular function at 10 weeks of age. This was accompanied by a marked decrease in caveolin-3 mRNA and protein levels when compared to non-TG control mice. The change in caveolin-3 expression was selective as levels of caveolin-1 and −2 did not change. Confocal imaging of myocytes isolated from A_1-AR TG mice demonstrated a loss of the plate like appearance of T-tubules. Caveolin-3 levels were also reduced in hearts from mice over-expressing TNFα. There was a direct relationship between caveolin-3 expression and fractional shortening in all mice that were studied ($r= 0.65$; $p<0.001$). Although we could not demonstrate a significant decrease in caveolin-3 levels in failing human heart, we did find a direct correlation ($r=0.7$; $p<0.05$) between levels of caveolin-3 protein and Ca^{2+}-ATPase, a marker of the heart failure phenotype. These results suggest a relationship between left ventricular dysfunction and caveolin-3 levels and suggest that caveolin-3 may provide a novel target for heart failure therapy.

Correspondence to: Arthur M. Feldman MD, PhD, Department of Medicine, Jefferson Medical College, 1025 Walnut, Street Suite 822 College Building, Philadelphia PA 19107, Fax: (215) 955-2318, Phone: (215) 955-6946, Arthur.Feldman@Jefferson.edu.

Disclosures: None

Keywords

heart failure; caveolin-3; adenosine receptor

Introduction

Caveolae are 50 to 100 nm flask-shaped lipid rafts that appear as invaginations of plasma membranes in almost all types of cells. In the heart, studies using fluorescent calcium probes demonstrate that calcium waves originate from caveolae rich areas on the surface of endothelial cells (1,2) and calcium channels and important cardiac regulatory proteins including G protein-coupled receptors have been localized to caveolae(3). The unique shape of caveolae is attributable to the presence of the scaffolding protein caveolin. When caveolin is expressed in the membrane it spontaneously organizes membrane lipids into caveolae. Caveolins also anchor receptors in the caveolae and are crucial in receptor internalization in response to ligand stimulation, in receptor recycling and in compartmentalization of downstream signals(4,5). Three distinct mammalian caveolin genes have been identified: Caveolins-1, −2, and −3. Caveolins-1 and −2 are expressed predominantly in endothelial cells and adipocytes while caveolin-3 is confined to skeletal, cardiac and smooth muscle.

While caveolin play a significant role in the physiology of the heart, studies designed to understand their role in cardiovascular pathophysiology have resulted in incongruent findings. Chronic hypoxia and chronic beta-adrenergic receptor stimulation result in down regulation of caveolin expression(6,7). In addition, caveolin-3 expression is decreased in a rat model of hypertension induced cardiomyopathy, and normalization of caveolin-3 levels was associated with improved exercise and regression of the hypertrophic phenotype(8). Consistent with the finding that caveolin-3 expression decreased in models of heart failure, genetic ablation of caveolin-3 in mice resulted in the development of a heart failure phenotype with hypertrophy, dilatation and reduced ventricular function(9). By contrast, Ohsawa *et al.*(10)described cardiac hypertrophy and enhanced contractility – not dilation and failure - in transgenic mice with a Pro104Leu mutation in caveolin-3. Dogs with pacing induced heart failure demonstrated increased levels of caveolin-3 protein(11). Similarly, failing human heart obtained at the time of the placement of a left ventricular assist device demonstrated increased caveolin-3 mRNA when compared with mRNA levels in non-diseased human heart tissue, although levels of caveolin-3 increased further after left ventricular unloading(12).

In order to better understand the relationship between left ventricular dysfunction and caveolin expression, we took advantage of two well-characterized murine models of left ventricular dysfunction: mice with constitutive (TG_{con}) or induced (TG_{ind}) cardiac-restricted over-expression of the A_1-adenosine receptor (A_1-TG) and mice with constitutive and cardiac-restricted over-expression of the pro-inflammatory cytokine tumor necrosis factor-α (TNF1.6)(13,14). We found that left ventricular dysfunction is associated with a profound and selective decrease in the expression of caveolin-3 protein and mRNA. This decrease was directly related to the degree of left ventricular dysfunction. While the molecular mechanism responsible for the decrease in caveolin-3 remains undefined, our results demonstrate that the decrease in caveoline-3 mRNA and protein is not attributable to changes in the expression of the obligate nuclear regulatory factor myogenin or to G-protein-coupled signaling pathways.

Methods

Transgenic mouse generation

Transgenic mice with constitutive (TG_{con}) and adult induced (TG_{ind}), cardiac-restricted over-expression of the human A_1-AR and A_{2A}-AR,, were generated as previously described (13,15). Doxycycline was deleted from the diet of pregnant breeders (TG_{con}) or from transgenic off-spring at 3 weeks of age (TG_{ind}). Transgenic mice with cardiac restricted overexpression of TNFα in FVB background, (TNF1.6) mice were generated as previously described(16). The A_1-AR mouse line was crossed with transgenic GiCT mice(17), animals with cardiac specific inducible inhibitor of αG_{i2} function, to generate the A_1GiCT triple transgenic mouse lines. All experimental animal protocols were approved by the Institutional Animal Care and Use Committee of Thomas Jefferson University.

Echocardiography

Two-dimensional transthoracic echocardiography was performed on WT and transgenic mice by use of the VisualSONICS VeVo 770 imaging system with a 707 scanhead. Left ventricular dimensions were measured in M-mode short-axis view in end diastole and end systole. Mice were lightly anesthetized with inhalation of isofluorane (1.5%), placed in supine position and restrained; total anesthesia duration did not exceed 5 minutes.

Real-Time Quantitative Polymerase Chain Reaction

cDNA was reverse transcribed from 1 ug of total RNA extracted from mouse left ventricles (n=5 per group) to determine expression of endogenous caveolin-3. Two sets of caveolin-3 primers were validated and used: Fj, 5′CCG AAG AGC ACA CAG ATC TGG-3′ (Exon 1) Rj/5′-GAG CAG GGC CAG TGG AAC ACC-3′ (Exon 2) and Fs, 5′-CTG CCC CCA GGA CTA TCA AC-3′ (Exon 1)/Rs, 5′-TTC CAG ATC CGT GTG CTC TTC-3′ (Exon 2). GAPDH and actin genes were used as a reference for normalization of obtained measurements. Analysis of gene expression level was performed using 2 (−delta delta C(T)) method(18).

Isolation and adeno-viral infection of adult murine cardiac myocytes

Adult myocytes were isolated as previously described(14). Briefly septum and left ventircular free wall from male 12–14 week TG hearts or wild-type non-transgenic control hearts were enzymatically digested with collagenases B and D and protease XIV. Isolated adult myocytes were plated on laminin-coated glass cover slips in a 6-well plate, and the Ca^{2+} concentration of the buffer was progressively increased from 0.05 to 0.125 to 0.25 to 0.5 mM in three steps (10 min interval each). The 0.5 mM Ca^{2+} buffer was then aspirated and replaced with minimal essential medium (MEM; Sigma M1018) containing 1.2 mM Ca^{2+}, Insulin-Transferrin-Selenium supplement (Invitrogen Corporation), 1% penicillin-streptomycin and 2.5% FCS. Cell culture was adjusted to pH 7.0 by the addition of $NaHCO_3$ (0.57g/l) and incubated in a 3.5% CO_2 incubator for 1hr. Then, cell culture medium was replaced with fresh medium without FCS and infected with either adenovirus (Adv) expressing green fluorescent protein (GFP) or Adv expressing both Caveolin-3 and GFP at a multiplicity of infection of 50. After 3hr incubation, viral media were removed and myocytes or H9C2 cells were cultured for 2 days.

Immunoblot Analysis

Left ventricular protein expression was detected by immunoblotting with an Odyssey Scanner (LI-COR, Lincoln, Nebraska). Left ventricular tissue was lysed with a modified RIPA Buffer (20mM Tris-HCl pH7.6, 137mM NaCl, 10% glycerol, 1%NP40, 0.1% SDS, 0.5% NaDeoxycholate) supplemented with protease and phosphatase inhibitors (in mM: 10

NaF, 10 PMSF, 1 NaVO4, 1 NapyroPO4, 1 EDTA, 1 DTT; 5ug/ml leupeptin and 5ug/ml aprotinin). 20 ug of protein lysates was separated by electrophoresis in a 4–12% Bis Tris Gel, transferred onto nitrocellulose, and probed with primary antibodies. Blots were subsequently incubated with secondary antibodies. Bands were visualized and directly quantified with the Odyssey v1.2 software. The following antibodies were used: anti-A_1-AR (Affinity BioReagents, Rockford, IL), anti-Cav1, Cav2, Cav3 (BD Transduction Laboratories, San Jose, CA), anti-pAkt, pErk, pJNK and p-P38 (Cell Signaling Tech., Beverly, MA), anti-myogenin and anti-ID2 (Santa Cruz Biotechnology, Santa Cruz, CA) and anti-GAPDH (Fitzgerald Industries International, Inc., Concord, MA), Secondary antibodies used: Goat Anti-Mouse Alexa Fluor 680 (Invitrogen, Carlsbad, CA) and IRDye 800 Goat Anti-Rabbit (Rockland, Gilbertsville, PA).

Immunofluorescence microscopy

Immunofluorescence myocyte staining, microscopy procedures and image acquisition were performed as previously described(14). The primary antibody used was anti-caveolin-3 (BD Transduction Laboratories, San Jose, CA). The secondary antibody used was Alexa-488 conjugated anti-mouse (Invitrogen, Carlsbad, CA) and 350 nmol/l DAPI nuclear stain (Invitrogen, Carlsbad, CA).

Myocyte T-tubule staining

Isolated myocytes were stained with di-8-ANEPPS (10 umol/l) at 37°C for 10 minutes. Stained myocytes were washed and examined by confocal microscopy (Zeiss LSM 510), using an excitation wavelength 488 nm/ emission wavelength 505 nm ratio.

Image Processing

Digital images of individual myocytes were processed using Fast Fourier Transform (FFT) algorithm to quantify the organization of caveolin-3 and T-tubule signal within cardiac myocytes. Each cell image was rotated horizontally to align periodic T-tubules in a vertical direction. The diffraction pattern with order spectra was displayed horizontally when FFT was performed on the image. Due to discontinuities and cell wall in the image, a small region of interest (200 × 60 pixels) with the best caveolin-3 and T-tubule image was selected from each image sample for WT and A_1-TG_{con} groups. The image contrast was enhanced by Unsharp Mask to increase acutance first and then the FFT algorithm was applied in IDL digital imaging software (Germantown, WI). Power spectrum in log scale vs. spatial frequency was calculated for each image.

Electron Microscopy

Hearts were collected from male 12–14 week wild type (n=3) and A_1-AR_{con} transgenic (n=3) mice and fixed in 2% paraformaldehyde, 2.5% glutaraldehyde in 0.1 M sodium cacodylate buffer, pH 7.4. After 15 minutes of initial fixation, a 1mm longitudinal slice and a 1 mm transverse slice were made through the left ventricle with the aid of Acrylic Heart Matrices (Harvard Apparatus, Holliston, MA). The tissue slices were further dissected and fixed for a total of 2 hours at room temperature. Post-fixation was performed with 1% osmium tetroxide in 0.1 M sodium odylate buffer, pH 7.4 for 1 hr, followed by dehydration through graded alcohols and propylene oxide. The samples were embedded in EMbed 812 (Electron Microscopy Sciences, Hatfield, PA). Longitudinal and transverse sections were cut on an UltraCut E ultramicrotome (Reichert-Jung now Leica, Wien, Austria) and stained with uranyl acetate and lead(19). Images were collected with an AMT XR41-B 4 megapixel camera on a Hitachi H-7000 electron microscope.

Human heart tissue analysis

Nonfailing (n=5) human hearts were obtained from unused organ donors with no history of cardiac dysfunction or coronary artery disease. Failing hearts (n= 19) were obtained from end stage cardiac transplant recipients with advanced ischemic or idiopathic dilated cardiomyopathies. The Institutional Review Board of Thomas Jefferson University, the University of Pittsburgh, and of University of Colorado Health Sciences Center approved the study. Approximately 100mg of left ventricular free wall tissues frozen at −80°C were extracted with 300ul of modified RIPA buffer (20mM Tris-HCl pH7.6, 137mM NaCl, 10% glycerol, 1%NP40, 0.3% SDS, 0.5% NaDeoxycholate supplemented with Thermo Fisher Scientific Halt Protease and Phosphatase Inhibitor Single-Use Cocktail). The homogenates were centrifuged at 13000 ×g for 20 minutes at 4°C. Protein were heated and denatured with sample buffer, then stored in −80°C for immunoblotting analysis. Total cardiac tissue homogenates (40 μg in a volume of 20 μL) were immunoblotted. Following antibodies were used: anti-caveolin-3 (BD Transduction Laboratories, CA), α1-H subunit of T-type calcium channel (Neuromab, UC Davis 75–095), anti-actin (Sigma-Aldrich, MO), and anti-GAPDH and caveolin-1 (Santa Cruz Biotech, CA).

Statistical Analysis

A commercial software package was used for statistical analysis (Graph Pad Software Inc. La Jolla, CA 92037 USA). Comparison of means ± SE was analyzed by non-parametric Mann-Whitney test. Non-parametric Spearman Rank test was used to correlate caveolin-3 expression and fractional shortening in mice. Multiple regression analysis was used to correlate human SERCA expression with caveolin-1, caveolin-3, α1H subunit of T-type calcium channel and actin. A p-value of < 0.05 was considered statistically significant.

Results

As we have demonstrated previously, mice constitutively overexpressing A_1-AR (A_1-TG_{con}) developed marked cardiac dilatation and a profound decrease in left ventricular contractility by 10 weeks of age. (Fig. 1A, and Table 1)(13). To test the hypothesis that abnormalities in cardiac function might be associated with changes in caveolin-3 protein, we assessed caveolin-3 protein and mRNA levels in 10-week-old WT and A_1-TG_{con} left ventricular myocardium. A_1-TG_{con} myocardium had significantly less caveolin-3 protein when compared with WT controls (Fig. 1B, WT 1.00±0.05 vs. A_1-TG_{con} 0.39±0.07, $p < 0.05$). However, no significant changes were seen in the levels of caveolin-1 or caveolin-2 protein (Data not shown). Similarly, levels of caveolin-3 mRNA were also reduced in A_1-TG_{con} myocardium (Fig. 1C). Immunofluoresence staining of caveolin-3 in isolated myocytes showed that while caveolin-3 in WT myocytes stained along the striated T-tubules system, Caveolin-3 in A_1-TG_{con} myocytes could not be visualized along the T-tubules (Fig. 1D).

Transmission electron microscopy was performed to evaluate the morphology of A_1-TG_{con} mice. Heart samples viewed in both longitudinal and transverse planes revealed distinctive dilatation of the T-tubules in the A_1-TG_{con} mice (Fig. 2A). Focal accumulations of membranous material in whirled and concentric formations (myelin figures) were also visualized in the A_1-AR transgenic hearts but not in the wild type controls (data not shown). To further evaluate T-tubule structure, T-tubules in live myocytes were marked with Di-8-ANNEPS - a membrane phospholipid binding dye. As seen in Fig. 2B, unlike T-tubules in WT myocytes, T-tubules in A_1-TG_{con} myocytes were not organized in a normal cross-striation pattern. We quantified abnormal T-tubule organization by Fourier transformation analysis. The distance between the zero- and first-order diffraction spots is inversely proportional to the length of repeating units in the grating, i.e., sarcomere length. Fourier transformation of Di-8-ANNEPS stained confocal images gave rise to a series of well-

defined diffraction spots in WT myocytes (Fig. 2B, lower panel). By contrast, first order diffraction spots were missing in cells from A_1-TG_{con} myocytes, suggesting that the T-tubules were disorganized.

The expression of the A_1-AR transgene can be inhibited by maintaining the mice on Doxycycline (Dox). Removal of Dox-containing diets from mice at 3-weeks-of-age induced A_1-AR gene expression at 6 weeks-of-age. At 10 weeks-of-age, mice with induced overexpression of A_1-AR (A_1-TG-$_{ind}$) had a fractional shortening (Figure 3A) similar to that of littermate controls. However, at 26 weeks-of-age, A_1-TG-$_{ind}$ mice demonstrated a significant decrease in left ventricular function (Fig. 3A and Table 1, FS% WT 47+/−2 vs. A1-TG_{ind} 30+/−2; $p<0.05$) that was similar to that seen in mice with constitutive overexpression of A1-AR. *As seen in* Figure 3B, 26 week-old A1-TG_{ind} *mice demonstrated a marked decrease in caveolin-3 expression, whereas aging of wild-type mice from 12 weeks to 26 weeks did not alter caveolin-3 expression.* Caveolin-3 levels were also reduced in mice overexpressing the pro-inflammatory protein tumor necrosis factor-α (Fig. 3C). These mice show a more modest decrease in left ventricular function than is found in mice with constitutive or induced expression of the A_1-AR. There was a statistically significant correlation ($r=0.65$; $p<0.001$) between fractional shortening and caveolin-3 expression in A_1-AR TG_{con}, A_1-AR_{ind}, TNFα, and appropriate age-matched and WT controls (Figure 3D).

As caveolins are known to regulate signal transduction, we determined activation status of signaling proteins, Akt, Erk, JNK and p38 in WT and A_1-TG_{con} left ventricular myocardium. Immunoblotting of these phospho-kinases showed that only phospho-Akt was reduced in an A_1-TG –dependent manner (Fig. 4A and 4B). To determine if Caveollin-3 expression was sufficient to rescue Akt activity in failing myocytes overexpressing A_1-AR, myocytes were isolated from 20-week-old WT and adult-induced A_1-R TG mice and infected with either Adv-Caveolin-3 or Adv-GFP. After culturing infected myocytes for 48 hours, cells were stimulated with insulin for 15 minutes. As seen in Fig. 4C, Caveolin-3 overexpression synergized with insulin to phosphorylate Akt and enhanced the phosphorylation of the Akt kinase target PRAS40 in myocytes isolated from A_1-TG mice ($n=4$, $p<0.05$).

To determine whether alterations of caveolin-3 expression and organization were specific to A_1-AR overexpression, we assessed caveolin-3 expression in mice overexpressing another adenosine receptor subtype, the A_{2A}-AR, at levels comparable to those seen in the A_1-TG_{con} model (13,14). In marked contrast to the constitutive overexpression of A_1-AR, overexpression of A_{2A}-AR did not result in changes in caveolin-3 protein levels (Figure 5A) or caveolin-3 expression pattern (Figure 5B). As we reported previously, co-overexpression of the A_1-AR and A_{2A}-AR at an equimolar ratio prevented the development of left ventricular dysfunction (Fig 5C) and these bi-transgenic animals did not demonstrate alterations in the levels of cavveolin-3 protein (Fig. 5A).

To understand whether the changes in caveolin-3 protein in murine models of heart failure were representative of changes that might occur in the failing human heart, we measured caveoline-3 expression in samples of failing human heart obtained at the time of cardiac transplantation and compared these with samples of non-failing human heart tissue obtained at the time of tissue harvest. *The mean age of the individuals from whom the non-failing hearts were harvested was 50.4 ± 3.0 n=5 while that of the transplant recipients was 54.7 ± 1.5 (n=20; p=NS)* There was a trend towards a decrease in caveolin-3 levels in failing human heart normalized to GAPDH (1.2+/−0.2 units) when compared with non-failing controls (1.9+/−0.6 units) but this trend did not reach statistical significance due to high variation within the heart failing group ($p = 0.24$). *The* Ca^{2+-} *ATPase (SERCA)/GAPDH ratio in the failing cohort (0.80+/−0.07, n=18) was significantly lower than in non-failing*

control hearts (1.14+/−0.07, n=5, p<0.05). We also found that there was a direct correlation between myocardial levels of caveolin-3 and SERCA, an established molecular marker of the heart failure phenotype (Fig. 6). Using multiple regression analysis, levels of caveolin-1, α1-H subunit of T-type calcium channel and actin did not correlate with levels of SERCA.

A_1-AR mediates at least some of its downstream effects by coupling with the inhibitory G protein, G_i. To test whether the A_1-AR mediated decrease in caveolin-3 expression was mediated by G_i, we created transgenic mice over-expressing both A_1-AR and a G_i-selective inhibitory peptide (GiCT). GiCT is comprised of the carboxyl-terminal 63 amino acids of G_{i2} to "functionally knock out" all GPCR-G_i–induced signals in the heart(17). As seen in Figure 7, mice that expressed both A_1-AR and GiCT demonstrated marked cardiac dilatation and diminished LV function when compared with A_1-TG_{ind} mice ($p<0.001$) suggesting that functional knockout of cardiac $G\alpha_i$ signaling (GiCT) could not rescue A_1-AR signaling induced cardiomyopathy. The transcription factor myogenin is both sufficient and necessary to activate caveolin-3 expression by binding to its regulatory binding site in the promoter region of the caveolin-3 gene. By contrast, the nuclear protein Id2 inhibits myogenin activity. We were not able to demonstrate changes in the levels of myogenin or Id2 protein in A_1-TG_{con} mice when compared with WT controls. (data not shown)

Discussion

In this study, we demonstrated that left ventricular dysfunction in mice over-expressing A_1-AR is associated with significantly reduced levels of caveolin-3 mRNA and protein. Confocal microscopy of isolated myocytes immunostained with caveolin-3 and Di-8-ANNEPS, showed abnormal caveolin-3 signal organization and T-tubules in myocytes isolated from A_1-AR TG mice. Similarly electron microscopy demonstrated T-tubule dilation with focal accumulation of membranous material. These changes are not selective for A_1-AR induced heart failure as abnormalities in caveolin-3 expression were also observed in a commonly studied form of murine heart failure: cardiomyopathy secondary to constitutive over-expression of TNFα(20) as well as in failing human heart. In transgenic mouse myocardium with augmented expression of the highly homologous A_{2A}-AR, caveolin-3 levels were normal, suggesting that decreased expression of caveolin-3 is unlikely to be due to overexpression of a G-protein coupled receptor per se. In addition, co-overexpression of the A_1- and A_{2A}-AR did not result in abnormalities in LV function or in caveiolin-3 expression or localization, and these animals had near normal ventricular function(14). Interestingly, inhibition of G_{i2} function (GiCT) did not rescue A_1-AR induced cardiomyopathy, suggesting that the change in caveolin-3 expression was not mediated by G_{i2}.

That changes in levels of caveolin-3 protein can alter cardiac function has been demonstrated in earlier studies. Both calcium cycling and A_1-AR have been previously localized to caveolae and functionally linked to caveolin-3. Calcium influx and regulation have been localized to caveolae in the myocardium(21). Studies using fluorescent calcium probes demonstrated that calcium waves originate from caveolae rich areas on the cell surface(1,2) and calcium channels and regulatory proteins have been localized to caveolae(3). Furthermore caveolins, the proteins that anchor receptors in the caveolae, are crucial in A_1-AR internalization in response to ligand stimulation, in receptor recycling and in its downstream signal compartmentalization(4,5). In fact, A_1-AR co-immunoprecipitated with caveolin-3 and likely localizes to caveolae in the cell membrane (4). Mice over-expressing TNFα also demonstrate profound changes in calcium homeostasis (22). Thus, the profound reduction in caveolin-3 levels in hearts of A_1-AR TG and TNF1.6 mice could contribute to ventricular dysfunction in both murine heart failure models.

We were unable to demonstrate a significant decrease in the levels of caveolin-3 in failing human heart when compared with non-failing controls. This was likely due to the heterogeneity that is found in both failing and "non-failing" human heart. However, we were able to demonstrate a highly significant and linear relationship between the levels of caveolin-3 and SERCA – an incontrovertible marker of the adult heart failure phenotype. This relationship was specific for caveolin-3 as a similar relationship could not be demonstrated with caveolin-1, actin, or α1-H subunit of T-type calcium channel.

Abnormalities in caveolin-3 expression have been previously associated with myocardial dysfunction but there are significant inconsistencies in the results. Caveolin-3 knock out mice developed a cardiomyopathic phenotype with significant hypertrophy, dilatation and reduced fractional shortening of the myocardium(9). Similarly, caveolin-3 expression was decreased in hypertension induced cardiomyopathy, and normalization of caveolin-3 levels was associated with improved exercise tolerance and regression of the hypertrophic phenotype in a rat model(8). By contrast, Ohsawa *et al.*(10)described hypertrophic cardiomyopathy and enhanced – not diminished - contractility in transgenic mice with a Pro104Leu mutation in caveolin-3. Similarly, Hayashi *et al.*(23) discovered a mutation in a residue involved in Limb Girdle Muscular Dystrophy, in a sibling case of hypertrophic cardiomyopathy. Both caveolin-1 and caveolin-3 protein levels increased in dogs with heart failure secondary to over-drive pacing as measured in arbitrary units on two Western blots and electron microscopy and two-photon imaging showed a normal striated pattern for caveolin-3 consistent with localization in T-tubules(11). Caveolin-3 mRNA levels were reported to be elevated in human heart tissue obtained at the time of placement of a left ventricular assist device when compared with non-failing controls(12). The disparities between the various data may be due to the use of different species, the failure to assess levels of protein (as versus levels of mRNA) or differences in the degree of left ventricular dysfunction seen in the different models. Unlike earlier studies, we utilized multiple heart failure models and varying degrees of left ventricular dysfunction which allowed us to demonstrate that changes in caveolin-3 expression are only identifiable in the late stage of left ventricular dysfunction.

That a decrease in caveolin-3 expression could fundamentally change the morphology of the heart was demonstrated by the finding that over-expression of A_1-AR and abnormal caveolin-3 were associated with disorganization of T-tubule structure as observed by confocal microscopy and T-tubule dilatation and focal accumulation of membranous material in dilated T-tubules as seen by electron microscopy. This finding is consistent with previous studies showing caveolin-3 is a crucial structural component of caveolae membranes and regulates membrane repair proteins such as dysferlin (24,25).

Overexpression of A_1-AR also results in a marked decrease in phosphorylated Akt. Phosphorylation of Akt protects the heart from injury during ischemia-reperfusion (26–28). Mice deficient in Akt subtypes demonstrate myocardial contractile dysfunction after constriction of the ascending aorta and enhanced apoptosis after ischemic injury (29,30). Our finding that overexpression of caveolin-3 in A_1-TG myocytes could effectively reverse the diminution in Akt phosphorylation suggests that the decrease in Akt phosphorylation in mice over-expressing the A_1-AR is secondary to a marked decrease in the level of caveolin-3. It remains to be determined whether this decrease in phosphorylation of Akt is the result of altered caveolin-3 signaling or due to an uncoupling of relevant signaling molecules from their target proteins due to changes in caveolae structure secondary to the marked decrease in caveolin-3 protein. Since several models of cardiomyopathy with disparate etiology, A_1-AR-overexpression and TNFα-overexpression, demonstrated reduced caveolin-3 expression. It is possible that reduced caveolin-3 and t-tubular disorganization may be a general pathologic mechanism in the progression of the heart failure phenotype.

Further evaluation of the complex pathways that regulate caveolin-3 expression and caveolin-3-dependent signaling may provide important new therapeutic insights.

Two findings suggest that left ventricular dysfunction results in altered caveolin-3 expression through a unique and as yet, undefined mechanism. First, functional inhibition of aG_{i1}, a primary pathway for A_1-AR signaling as well as for regulating gene expression, failed to attenuate the effects of A_1-AR over-expression on levels of caveolin-3. Second, the decrease in caveolin-3 expression in mice with left ventricular dysfunction was not associated with changes in the level of myogenin, a transcription factor that is both sufficient and necessary for activation of caveolin-3 expression nor did it alter levels of Id2, a nuclear protein that regulates myogenin activity (31). Since we saw parallel changes in both caveolin-3 mRNA and protein, it is unlikely that these changes can be attributable to post-translational modification. One possible mechanism is that caveolin-3 gene transcription is differentially regulated in heart failure by micro RNAs. Further studies will be required to test this hypothesis.

Conclusion

The results of the present study demonstrate that the heart failure phenotype in A_1-AR over-expressing transgenic mice and in mice over-expressing TNFα is associated with a marked decrease in myocardial levels of caveolin-3, and loss of T-tubule structural integrity. Taken together, these results suggest that caveolin-3 may be a novel therapeutic target in patients with heart failure.

Acknowledgments

Funding Sources: This work was supported by the National Heart, Lung and Blood Institute grant HL 091799-01 (AMF), HL 061690, HL 085503, HL 075443 (WJK), HL 58672, HL 74854 (JYC).

References

1. Isshiki MAR. Calcium signal transduction from caveolae. Cell Calcium. 1999; 26:201–8. [PubMed: 10643558]
2. Isshiki MAJ, Yamamoto K, Fujita T, Ying Y, Anderson RGW. Sites of Ca(2+) wave initiation move with caveolae to the trailing edge of migrating cells. J Cell Sci. 2002; 115:475–84. [PubMed: 11861755]
3. Fujimoto T. Calcium pump of the plasma membrane is localized in caveolae. J Cell Biol. 1993; 120:1147–57. [PubMed: 8382206]
4. Lasley RDNP, Uittenbogaard A, Smart EJ. Activated cardiac adenosine A1 receptors translocate out of caveolae. J Biol Chem. 2000; 275:4417–21. [PubMed: 10660613]
5. Escriche MBJ, Ciruela F, Canela EI, Mallol J, Enrich C, Lluis C, Franco R. Ligand-induced caveolae-mediated internalization of A1 adenosine receptors: morphological evidence of endosomal sorting and receptor recycling. Experimental Cell Research. 2003; 285:72–90. [PubMed: 12681288]
6. Oka N, Asai K, Kudej RK, Edwards JG, Toya Y, Schwencke C, et al. Downregulation of caveolin by chronic beta-adrenergic receptor stimulation in mice. Am J Physiol. 1997 Dec; 273(6 Pt 1):C1957–62. [PubMed: 9435501]
7. Shi Y, Pritchard KA Jr, Holman P, Rafiee P, Griffith OW, Kalyanaraman B, et al. Chronic myocardial hypoxia increases nitric oxide synthase and decreases caveolin-3. Free Radic Biol Med. 2000 Oct 15; 29(8):695–703. [PubMed: 11053770]
8. Lee YI, Cho JY, Kim MH, Kim KB, Lee DJ, Lee KS. Effects of exercise training on pathological cardiac hypertrophy related gene expression and apoptosis. Eur J Appl Physiol. 2006 May; 97(2): 216–24. [PubMed: 16583233]
9. Woodman SEPD, Cohen AW, Cheung MWC, Chandra M, Shirani J, Tang B, Jelicks LA, Kitsis RN, Christ GJ, Factor SM, Tanowitz HB, Lisanti MP. Caveolin-3 knock-out mice develop a progressive

cardiomyopathy and show hyperactivation of the p42/44 MAPK Cascade. J of Biol Chem. 2002; 277:38988–97. [PubMed: 12138167]

10. Ohsawa YTH, Katsura M, Morimoto K, Yamada H, Ichikawa Y, Murakami T, Ohkuma S, Komuro I, Sunada Y. Overexpression of P104L mutant caveolin-3 in mice develops hypertrophic cardiomyopathy with enhanced contractility in association with increased endothelial nitric oxide synthase activity. Human Mol Genetics. 2004; 13:151–7.
11. Hare JMLR, Juang GJ, Colman L, Ricker KM, Kim B, Senzaki H, Cao S, Tunin RS, Kass DA. Contribution of caveolin protein abundance to augmented nitric oxide signaling in conscious dogs with pacing induced heart failure. Circ Res. 2000; 86:1085–92. [PubMed: 10827139]
12. Uray IP, Connelly JH, Frazier OH, Taegtmeyer H, Davies PJ. Mechanical unloading increases caveolin expression in the failing human heart. Cardiovasc Res. 2003 Jul 1; 59(1):57–66. [PubMed: 12829176]
13. Funakoshi HCT, Good JC, Libonati JR, Piuhola J, Chen X, MacDonnell S, Lee LL, Herrmann DE, Zhang J, Martini J, Palmer TM, Sanbe A, Robbins J, Houser SR, Koch WJ, Feldman AM. Regulated overexpression of the A1-adenosine receptor in mice results in adverse but reversible changes in cardiac morphology and function. Circulation. 2006; 114:2240–50. [PubMed: 17088462]
14. Chan TOFH, Song J, Zhang X, Wang J, Cheung PH, DeGeorge BR Jr, Li X, Zhang J, Herrmann DE, Diamond M, Houser SR, Koch WJ, Cheung JY, Feldman AM. Cardiac-Restricted Overexpression of the A2A-Adenosine Receptor Increases Contractile Performance in Mice By Altering Calcium Handling. Clinical and Translational Science. 2008; 1:126–33. [PubMed: 20354569]
15. Sanbe AGJ, Hanks MC, Liang Q, Osinska H, Robbins J. Reengineering inducible cardiac-specific transgenesis with an attenuated myosin heavy chain promoter. Circ Res. 2003; 92(6):609–16. [PubMed: 12623879]
16. Kubota TMC, Frye CS, Slawson SE, Lemster BH, Koretsky AP, Demetris AJ, Feldman AM. Dilated cardiomyopathy in transgenic mice with cardiac-specific overexpression of tumor necrosis factor-alpha. Circ Res. 1997; 81:627–35. [PubMed: 9314845]
17. DeGeorge BRGE Jr, Boucher M, Vinge LE, Martini JS, Raake PW, Chuprun JK, Harris DM, Kim GW, Soltys S, Eckhart AD, Koch WJ. Targeted Inhibition of Cardiomyocyte Gi Signaling Enhances Susceptibility to Apoptotic Cell Death in Response to Ischemic Stress. Circulation. 2008; 117:1378–87. [PubMed: 18316484]
18. Livak KJST. Analysis of relative gene ex pression data using real-time quantitative PCR and the 2(-Delta Delta C(T) Method. Methods. 2001; 25:402–8. [PubMed: 11846609]
19. Sato T. A modified method for lead staining of thin sections. J Electron Microsc. 1968; 17:158–9.
20. Feldman AM, Combes A, Wagner D, Kadakomi T, Kubota T, Li YY, et al. The role of tumor necrosis factor in the pathophysiology of heart failure. J Am Coll Cardiol. 2000 Mar 1; 35(3):537–44. [PubMed: 10716453]
21. Cavalli AEM, Minosyan TY, Stefani E, Philipson KD. Localization of sarcolemmal proteins to lipid rafts in the myocardium. Cell Calcium. 2007; 42:313–22. [PubMed: 17320949]
22. London B, Baker LC, Lee JS, Shusterman V, Choi BR, Kubota T, et al. Calcium-dependent arrhythmias in transgenic mice with heart failure. Am J Physiol Heart Circ Physiol. 2003 Feb; 284(2):H431–41. [PubMed: 12388316]
23. Hayashi TAT, Ueda K, Shibata H, Hohda S, Takahashi M, Hori H, Koga Y, Oka N, Imaizumi T, Yasunami M, Kimura A. Identification and functional analysis of a caveolin-3 mutation associated with familial hypertrophic cardiomyopathy. Biochem and Biophys Research Communication. 2004; 313:178–84.
24. Hernandez-Deviez DJHM, Laval SH, Bushby K, Hancock JF, Parton RG. Caveolin regulates endocytosis of the muscle repair protein, dysferlin. The Journal of Biological Chemistry. 2008; 283:6467–88. [PubMed: 18171675]
25. Ishikawa H. Formation of elaborate networks of T-system tubules in cultured skeletal muscle with special reference to the T-system formation. J of Biol Chem. 1968; 38:51–66.

26. Fujio Y, Nguyen T, Wencker D, Kitsis RN, Walsh K. Akt promotes survival of cardiomyocytes in vitro and protects against ischemia-reperfusion injury in mouse heart. Circulation. 2000 Feb 15; 101(6):660–7. [PubMed: 10673259]

27. Matsui T, Tao J, del Monte F, Lee KH, Li L, Picard M, et al. Akt activation preserves cardiac function and prevents injury after transient cardiac ischemia in vivo. Circulation. 2001 Jul 17; 104(3):330–5. [PubMed: 11457753]

28. Miao W, Luo Z, Kitsis RN, Walsh K. Intracoronary, adenovirus-mediated Akt gene transfer in heart limits infarct size following ischemia-reperfusion injury in vivo. J Mol Cell Cardiol. 2000 Dec; 32(12):2397–402. [PubMed: 11113015]

29. DeBosch B, Sambandam N, Weinheimer C, Courtois M, Muslin AJ. Akt2 regulates cardiac metabolism and cardiomyocyte survival. J Biol Chem. 2006 Oct 27; 281(43):32841–51. [PubMed: 16950770]

30. DeBosch B, Treskov I, Lupu TS, Weinheimer C, Kovacs A, Courtois M, et al. Akt1 is required for physiological cardiac growth. Circulation. 2006 May 2; 113(17):2097–104. [PubMed: 16636172]

31. Biederer CHRS, Moser M, Florio M, Israel MA, McCormick F, Buettner R. The basic helix-loop-helix transcription factors myogenin and Id2 mediate specific induction of caveolin3 gene expression during embryonic development. J of Biol Chem. 2000; 275:26245–51. [PubMed: 10835421]

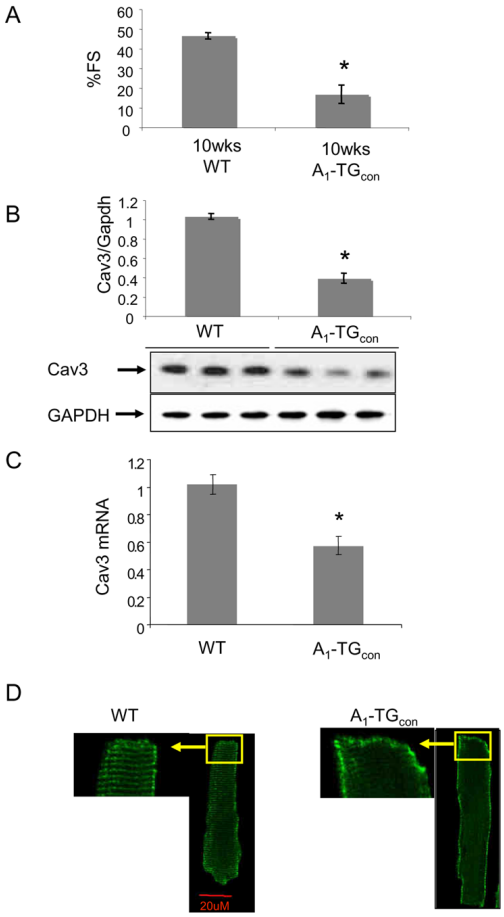

Figure 1.

(A) Fractional shortening percentage (%FS) measurement by echocardiograph. 10 week-old WT and A_1-TG_{con} mice were used (N=5-8). **P*<0.01. (B) Caveolin-3 protein expression. Ventricular extracts from 10 week-old mice were probed with indicated antibodies. Signals were normalized to GAPDH expression in WT hearts (N=5) and were analyzed by non-parametric method. Analyzed values were mean+/−SE, **P*<0.05 vs WT. (C) Reverse-transcribed total RNA from mouse left ventricles were used to detect caveolin-3 and GAPDH gene expression. Signals were normalized to GAPDH expression in WT hearts (N=5) and were analyzed by non-parametric method. Analyzed values were mean+/−SE, **P*<0.05 vs WT. (D) Immunofluorescence caveolin-3 staining of isolated myocytes. 600X confocal images represent at least 3 mice/genotype group and minimum 20 myocytes/mice examined. myocytes pooled from 4-5 mice/genotype group.

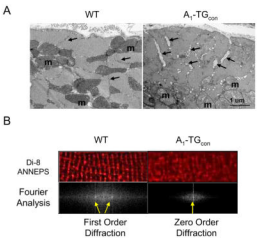

Figure 2.

A. Electron microscopy images of myocardial sections of male 12–14 week WT (n=3) and A_1-TG_{con} (n=3) mouse hearts. T-tubules (arrows) are dilated in the transgenic cardiac muscle. The dilated T tubules contain membranous and basement membrane-like material; m=mitochondrion. Bar = 1 micron. B. T-tubules were stained with the voltage sensitive lipid dye, di-8-ANNEPS, in live WT and A_1-TG_{con} myocytes. Confocal digital images were processed using Fast Fourier Transform (FFT) algorithm to quantify organization of T-tubule within myocytes. The power spectrum in log scale vs spatial frequency was calculated for each image and indicated by the appearance of zero or first order diffraction spots (arrows).

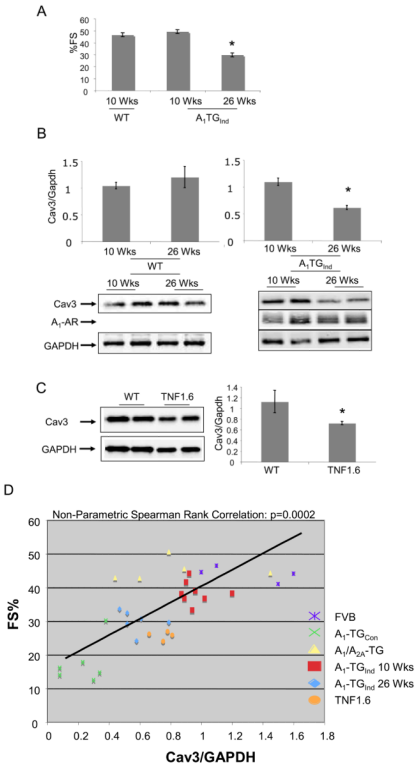

Figure 3.

(A) Adult A_1-AR induction. Doxycycline (DOX) was removed from transgenic mice at 3 weeks of age to induce A_1-AR expression (A_1-TG_{Ind}). Percent fractional shortening (%FS) were determined in A_1-TG_{Ind} mice at 10 week-of-age and at 26 week-of-age. *P<0.05 vs 10 week-old A_1-TG_{Ind}. *(B) Caveolin-3, A_1-AR and GAPDH expression in 10–12 week-old WT (N=8), 20–26 week-old WT (N=4), 10–12 week-old A_1-TG_{ind} (N=4) and 20–26 week-old A_1-TG_{ind} (N=8) mouse left ventricles. Data shown are mean +/− SE. *p<0.05. (C)* Caveolin-3 and GAPDH expression in 12 week-old WT and TNF 1.6 left ventricular tissues (N=4). Data shown are mean +/− SE. *p<0.05. (D) Cardiac function (FS%) and caveolin-3 protein expression were obtained from mice with the following genotypes: WT FVB mice (N=4), 10 wk-old A_1-TG_{con} (N=6), 10 wk-old A_1-TG_{Ind} (N=8), 26 wk-old A_1-TG_{Ind} (N=6), 10 wk-old A_1/A_{2A}-TG_{con} (N=5), TNF 1.6 (N=4). Non-parametric Spearman Rank test was used to correlate Cav3 expression with fractional shortening. Graph showed FS% and Caveolin-3/GAPDH scatter plot. Linear trend bar showed the significant correlation between caveolin-3 expression and fractional shortening (r=0.65; p<0.001).

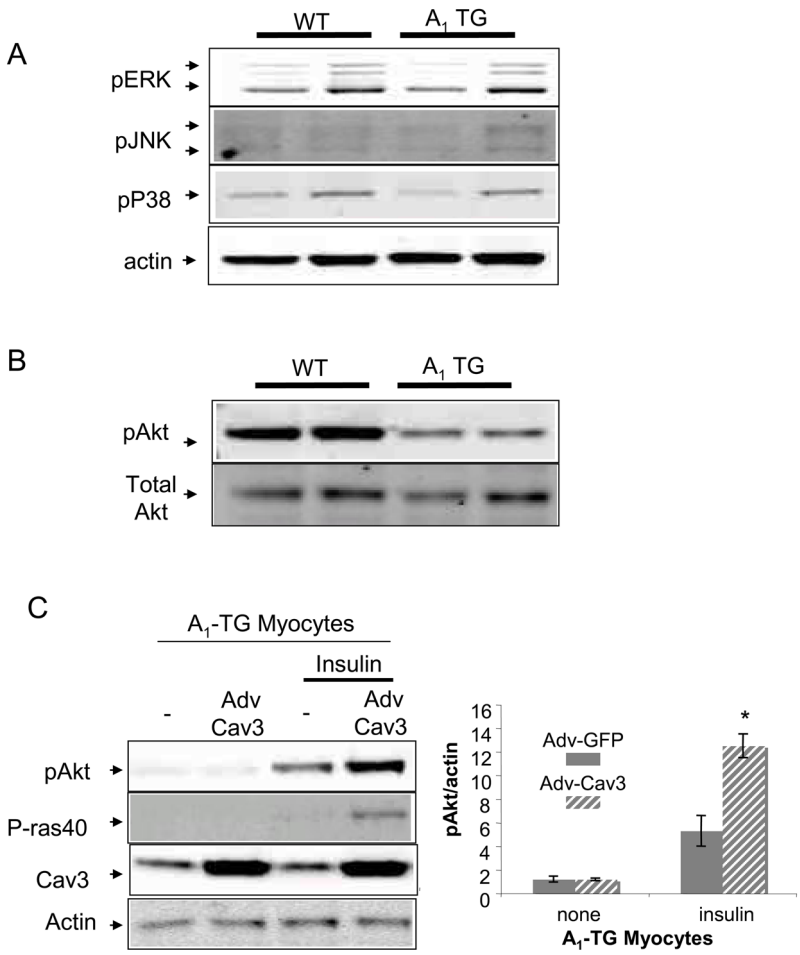

Figure 4.

Signal transduction in A1-TG hearts. (A) Extracts of 10 week-old WT and A_1-TG mouse left ventricles were probed with antibodies specific for Phospho-ERK, phospho-JNK and phospho-p38. (B) Extracts of 10 week-old WT and A_1-TG mouse left ventricles were probed with antibodies specific for Phospho-Akt and total Akt. (C) Adv-Caveolin-3 expression in A1-TG myocytes. Adult myocytes were isolated from 20-week-old adult induced A_1-TG mice. After infecting cells with Adv-Caveolin-3 virus or control Adv-GFP virus, myocytes were cultured for 48hrs. Then, cells were acutely stimulated with serum-free medium containing the Insulin-Transferrin-Selenium supplement (Invitrogen Corporation) for 15 minutes and probed with indicated antibodies. Blots shown were representative of at least three independent experiments. The graph showed pAkt/actin ratio: mean +/− SE. *$p<0.05$.

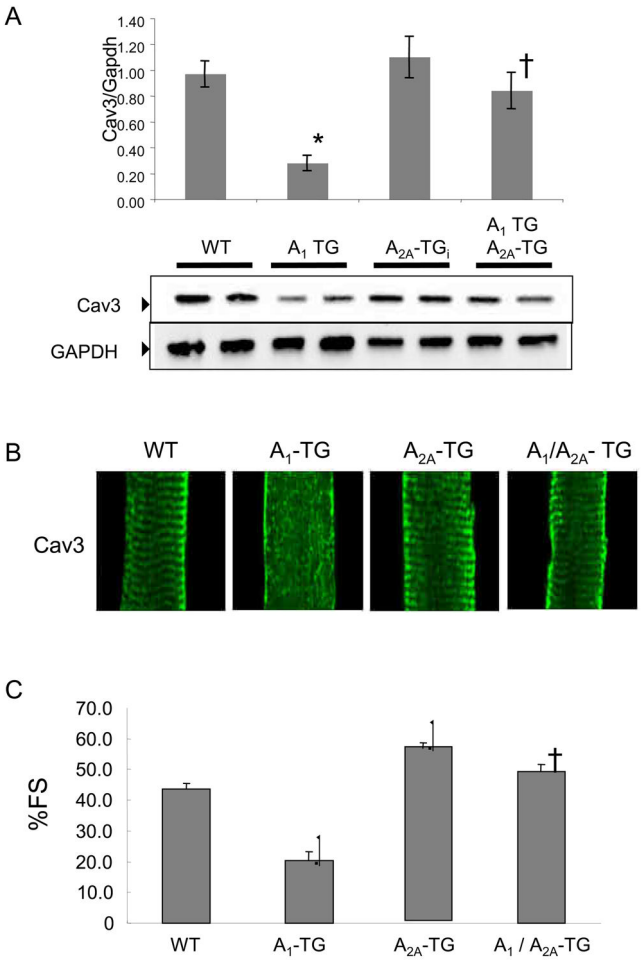

Figure 5.

Caveolin (Cav-3) protein expression, caveolin-3 localization and cardiac function in transgenic mice overexpressing both A_1-R and A_{2A}-R. (A) caveolin-3 expression in WT, A_1-TG, A_{2A}-TG and A1/A_{2A}-TG mice. Ventricular extracts from 10-week-old age and sex matched mice (N=4) were probed with indicated antibodies. Signals were normalized to GAPDH expression in WT hearts and were analyzed by non-parametric method. Analyzed values were mean+/-SE, **P*<0.05 vs WT. (B) Caveolin-3 localization in cardiac myocytes. 600X confocal images are shown. **(C)** Percent fractional shortening (%FS) of indicated mouse groups. **P*<0.001 vs WT, †*P*<0.001 vs A_1TG. (n=15–21, SE, male 8–12 week old mice).

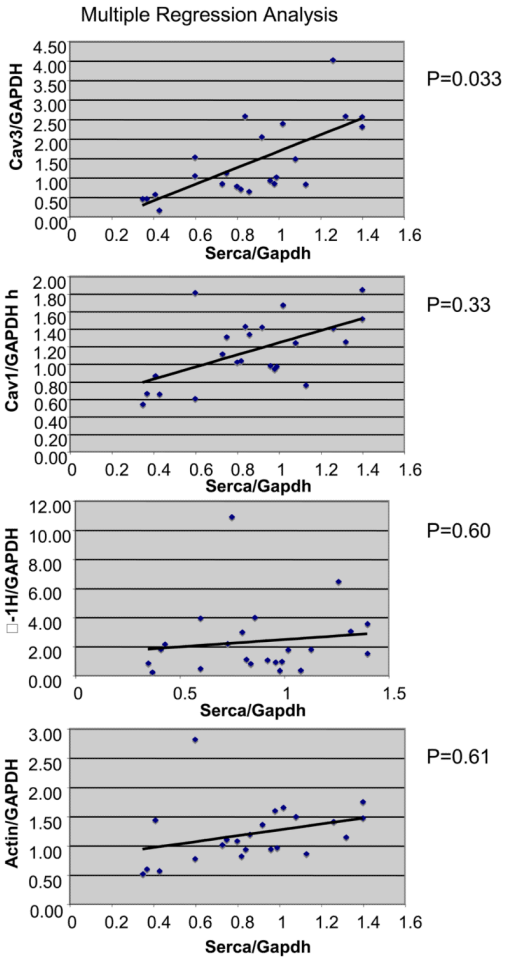

Figure 6.

Correlation of SERCA expression with caveolin-1, caveolin-3, α1-H and actin expression in human failing hearts. Caveolin-1, caveolin-3, SERCA, α1-H and actin expression were measured in 5 normal human hearts and 19 hearts from heart failure patients. GAPDH-normalized SERCA expression in each heart was compared to the expression of other proteins by multiple regression analysis. Scatter plots with correlation trend bars indicated the following p values: Serca vs Caveolin-3, $p<0.05$. Serca vs Caveolin-1, $p=0.34$; Serca vs α1-H, $p=0.60$; Serca vs actin, $p=0.61$.

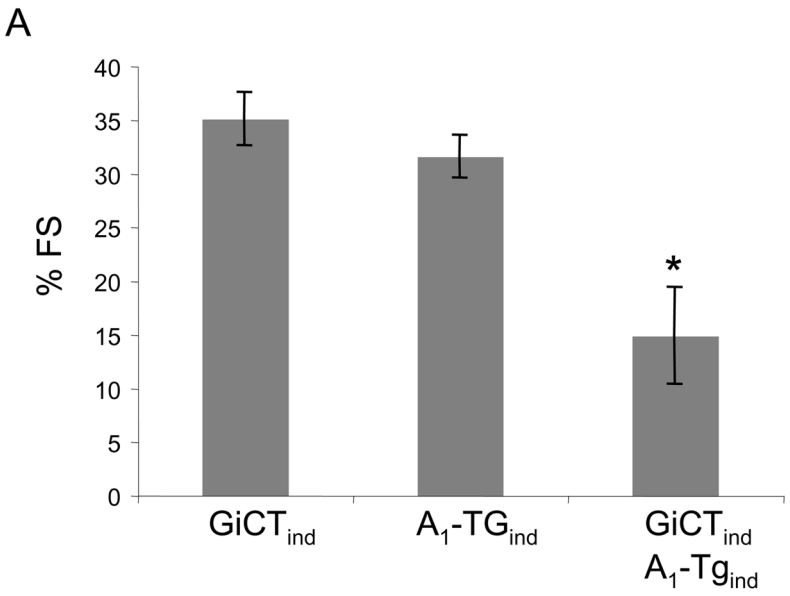

Figure 7.

Fractional shortening percentage (%FS) measurements of GiCT-TG_{ind}, A_1-TG_{ind}, and A_1/GiCT- TG_{ind} mice at 26 weeks-of-age, N=5 per group. Values are means +/− SE. *P<0.05 versus A_1-TG_{ind}.

Table 1

Echocardiography Data of WT, A_1-TGcon and A_1-TG_{ind} Mice

	WT (10wks)	**A_1-TG_{ind} (10wks)**	**A_1-TGind (26wks)**	**A_1-TG_{con} (10wks)**
N	8	10	6	5
HR (bpm)	441 ± 16	316 ± 24**	151 ± 7**	162 ± 13**
FS%	46.5 ± 1.7	49.2 ± 2.6	29.7 ± 1.6*	16.8 ± 4.7**
LVEDD (mm)	2.84 ± 0.11	3.18 ± 0.11	4.91 ± 0.24**	4.91 ± 0.21**
LVESD (mm)	1.53 ± 0.08	1.64 ±0.13	3.45± 0.24**	4.10 ± 0.36**

Echocardiography of male wild type and mice constitutively expressing A_1-AR (A_1-TG_{con}) and after DOX was removed from their diet at 3 weeks to induce myocardial A_1-AR expression (A_1-TG_{ind}). Echocardiography data: HR, heart rate; FS%, percent fractional shortening; LVEDD, LV end-diastolic dimension in mm; LVESD, LV end-systolic dimension in mm. Values are means +/− SEM.

* P<0.01 vs. WT and

** P<0.001 vs. WT